Biophysics and Physicobiology

https://www.jstage.jst.go.jp/browse/biophysico/

Review Article (Invited)

Methods to spontaneously generate three dimensionally arrayed microdroplets triggered by capillarity for bioassays and bioengineering

Hiroki Yasuga

Sensing System Research Center, National Institute of Advanced Industrial Science and Technology (AIST), Tsukuba, Ibaraki 305-8564, Japan

Herein, I review our recent work toward developing methods for generating three-dimensional (3D) droplet arrays driven by capillarity. Microdroplet array-based systems are useful for bioassays and bioengineering because they require only small amounts of samples and reagents and provide the high throughput. Various methods have been developed for preparing droplet arrays, among which methods based on capillarity have attracted considerable attention owing to their simplicity. I and collaborators have developed such methods based on capillary flow, including a method for preparing droplet arrays via oil–water replacement. We recently proposed our own concept of "fluid–fluid interfacial energy driven 3D structure emergence in a micropillar scaffold (FLUID3EAMS)" and its application. FLUID3EAMS allows a 3D droplet (or hydrogel bead) array to be generated in a micropillar scaffold by passing a fluid–fluid interface through the scaffold. This approach is useful for applications requiring ordered or arrayed microdroplets in biosensors, biophysics, biology, and tissue engineering. This review is an extended version of the article "FLUID3EAMS: Fluid–Fluid Interfacial Energy Driven 3D Structure Emergence in a Micropillar Scaffold and Development in Bioengineering" published in Seibutsu Butsuri (vol. 62, p. 110–113, 2022).

◀ *Significance* ▶

Methods for spontaneously generating microdroplets facilitate the preparation of droplet arrays, which broadens the applicability of droplet array-based systems. I and collaborators have been developing novel methods for generating microdroplet arrays based on capillary flow. This review introduces our recent achievements regarding methods for generating two-dimensional droplet arrays, as well as three-dimensional droplet arrays, which cannot be obtained via existing techniques.

Introduction

With the recent development of microfabrication technology, it has become possible to fabricate microscale structures with high precision. Microfluidic devices, which consist of microchannels prepared using microfabrication technology, allow the precise manipulation of small amounts of liquid [1]. Among the various types of microfluidic systems, droplet

Corresponding author: Hiroki Yasuga, Sensing System Research Center, National Institute of Advanced Industrial Science and Technology (AIST), 1-2-1 Namiki, Tsukuba, Ibaraki 305-8564, Japan. ORCID iD: https://orcid.org/0000-0003-2040-9017, e-mail: yasuga.h@aist.go.jp

microfluidics are capable of generating water-in-oil droplets with high reproducibility by utilizing the viscosity and interfacial tension, both of which are dominant at the microscale [2]. In chemical or biological analysis, it is possible to significantly reduce the amounts of samples and reagents needed and to yield a high throughput by using microscale droplets (microdroplets) generated in a microfluidic device as an individual chemical reactor. Although the analysis of microdroplets was proposed more than 50 years ago, it has only recently been achieved owing to developments in microfabrication technology [3]. Microdroplet-based systems have various applications, such as cell analysis, protein crystallization, and digital polymerase chain reactions [4].

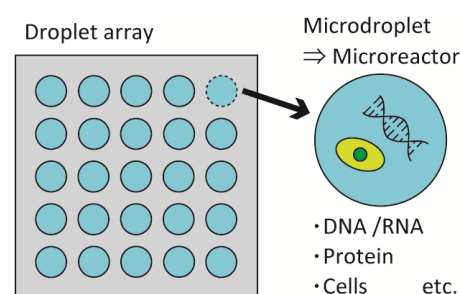**Figure 1** Conceptual drawing of assays based on droplet arrays.

A two-dimensional (2D) array of microdroplets facilitates the observation of droplets over time, increasing the experimental efficiency (Fig. 1). There are many different methods for arraying microdroplets. The simplest method is to pack the microdroplets generated in the device within a narrow planar microchamber [5]. However, the direct contact of microdroplets can cause stability problems such as droplet fusion and cross-contamination. The physical separation of microdroplets is an effective solution to this problem. For example, a method for immobilizing microdroplets in 2D or 2.5D structures in microfluidic devices [6] and a method for generating and arraying microdroplets directly using a robot-controlled dispenser [7,8] have been proposed. Compared with methods that involve preparing droplets one-by-one using robot-controlled dispensers, microfluidic approaches do not require individual control of droplets for arraying and thus allow rapid, automated droplet-array preparation. However, in automated microfluidic systems, syringe pumping is needed, which can degrade the properties of microsystems.

In recent years, methods have been proposed to generate and array microdroplets in a simple manner by utilizing the phenomenon that occurs when two mutually immiscible fluid interfaces pass through the microstructure. For example, in the "self-digitization" method proposed by Cohen et al., an array of microdroplets is generated by splitting an aqueous solution by passing an oil–water interface through microfluidic channels, including continuous bypass channels [9]. Although the "self-digitization" method requires a syringe pump to drive the interface, simplified methods utilizing the wettability or capillary flow have been proposed. Through the passage of the water–air interface through a well array template, an array of spatially separated aqueous solutions was obtained in an open environment [10]. Additionally, surface energy patterning is effective for the spontaneous generation of separated liquid columns in open environments [11–14]. These methods have the significant advantage of eliminating complex fluid manipulations such as pump operations. I and collaborators have also developed methods to generate droplet arrays utilizing the capillary flow that occurs spontaneously, e.g., the generation of droplet arrays via oil–water replacement in a circular well array with well-to-well connecting channels [15]. This method is possibly superior to the others because rough manipulation of the liquid, i.e., pipetting by hand, is sufficient to generate droplet arrays. In addition, the method of forming droplet arrays in a three-dimensional (3D) space has been considered for achieving high-density droplet arrays and expanding the application scope of the arrays [16]. I and collaborators developed a novel approach for generating 3D droplet arrays via capillarity-based oil–water replacement, which is referred to as fluid–fluid interfacial energy driven 3D structure emergence in a micropillar scaffold (FLUID3EAMS) [17,18].

The objective of this paper is to review the methods for spontaneous generation of droplet arrays, with a focus on our recent achievements. This paper introduces the basic principles, characteristics, and potential applications of FLUID3EAMS.

Capillarity-Based Droplet Generation and Manipulation

Capillarity is a useful phenomenon for microfluidics because the capillary flow of a liquid functions as a pressure source for microfluidic devices, resulting in a pumpless microfluidic system, which can be referred to as capillary or open microfluidics [19–21]. One typical phenomenon of capillary flow is that a narrow glass capillary draws water as soon as the capillary comes into contact with liquid water. Capillary flow is generated when the surface tension of a liquid, microstructure, and surface chemistry of the channels satisfy certain conditions, and it can be observed in various microstructures. Paper and porous materials can generate capillary flow, which has been commercially exploited for point-of-care testing, e.g., pregnancy tests [22]. However, the non-uniform microstructure of these materials poses problems regarding the reproducibility of capillary flow. Recent developments in microfabrication technology have allowed well-defined microstructures to generate capillary flows with good reproducibility [23]. For example, straight channels induce a predictable capillary flow inside the channel [24]. As another example, repetitive microstructures such as an array of posts or pillars can function as a capillary pump (sometimes called a "pillar forest"), as shown in Fig. 2(a). If the surface of the pillar forest is wettable by the liquid of interest, the liquid starts to flow inside the pillar forest once it comes into

contact with the pillar forest (Fig. 2(b)) [25]. As a pillar forest-based device, Zimmermann et al. designed capillary pumps composed of arrayed posts, lines, or more complex structures and demonstrated control of the capillary flow [26]. Bioassays using capillary flow have been extensively demonstrated in the form of lateral flow tests, which have been used for the detection of various biomarkers, including cardiac biomarkers [27,28].
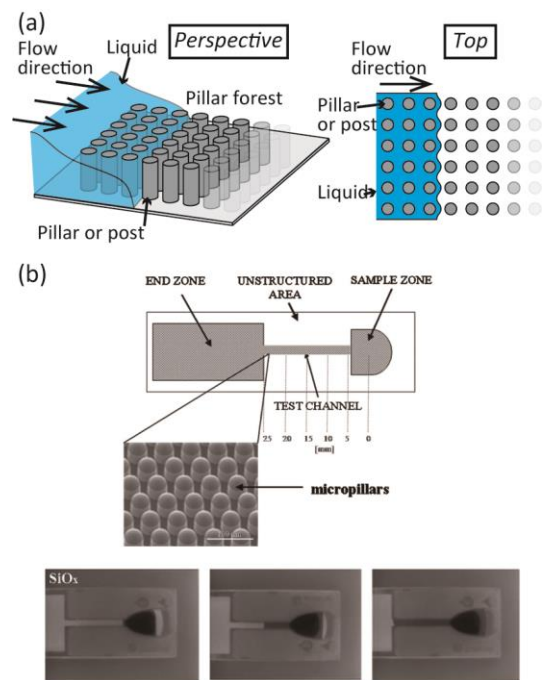
While most capillarity-driven microfluidic devices involve a single liquid spontaneously flowing through dry microstructures, spontaneous replacement between two mutually immiscible liquids, such as water and oil, has attracted attention. When a microstructure is filled with liquid A and is more wettable by liquid B than liquid A, liquid B replaces liquid A in the structure once the capillary comes into contact with liquid B [29]. Here, the spontaneous replacement between two liquids is termed as capillary replacement. A system based on capillary replacement is important for combining microdroplet-based systems with the capillary phenomenon. The combination can realize the generation of microdroplets without external pressure sources. Regarding droplet generation, it is difficult to drive ordinary droplet generators, such as those based on flow focusing [30] or T-junctions [31], because the flow rate of the capillary flow decreases over time [32]. To overcome this issue, I and collaborators developed a system to generate droplets by combining the self-digitization concept and the spontaneous replacement of oil and water [15]. A connected well array was proposed in which 2D-arrayed circular wells were connected in the column and row directions through a narrow channel, as

Figure 2 Capillary flow in pillar forests (an array of pillars or posts). (a) Schematic of capillary flow into a pillar forest. (b) Capillary flow in polymer-based pillar forests for lateral flow tests. Adapted from [25], copyright 2009, with permission from John Wiley and Sons.

shown in Fig. 3(a). The droplet array was generated as follows. First, an aqueous solution was deposited into the connected well array; then, an oil solution was applied to the array. Because the well array surface was more wettable by the oil solution, the oil solution spontaneously spread over the array and split the connection of the aqueous solution at the channel between two adjacent wells, forming a 2D droplet array. This system does not require an external pressure source to drive the flow, and droplets are generated automatically. In addition, there is a unique feature that the connected aqueous solution is turned into a droplet array by one drop of oil solution, which allows the production of droplet arrays with diffusively formed concentration gradients of a dual-sample solution. The utility of this feature for bioassays was validated through a live–dead cell assay, as shown in Fig. 3(b). The droplets in the aforementioned example were submillimeter-scale, but further miniaturization has been demonstrated using soft lithography [33].

Attempts have been made to realize an entire platform of droplet microfluidics with capillary flow. For droplet microfluidics, it is necessary to implement various elemental functions, such as transport, merging, and splitting of droplets, in addition to droplet generation, which is the most important function [34]. Toward droplet microfluidics driven by capillary flow, transport [35] and merging/splitting of droplets [21] have been implemented through the design of open channels and optimization of liquid selections (Fig. 3(c)) [36].

The multiphase capillary flow can be extended to other unique functionalities. For example, a constant capillary flow independent of the viscosity and surface energy of the sample liquid was demonstrated via the elaborate design of microchannels, with a focus on the effect of the displaced fluid [37,38]. As this example, further study on the capillarity between multiphase fluids will open up new possibilities for microfluidic devices that cannot be achieved by single-fluid capillary flow.

Droplet Generation by FLUID3EAMS

As highlighted in previous chapters, capillarity allows the spontaneous generation of a 2D droplet array. Recently, methods to generate droplet arrays in a 3D space have been discussed for increasing the density of droplet arrays or for more sophisticated applications [4,39]. However, the current methods are limited to techniques such as packing microdroplets into a chamber and arranging them in the 3D space [16]. To generate stable 3D droplet arrays, 3D structural templates are required for the physical separation of individual droplets, and methods for generating and arraying droplets
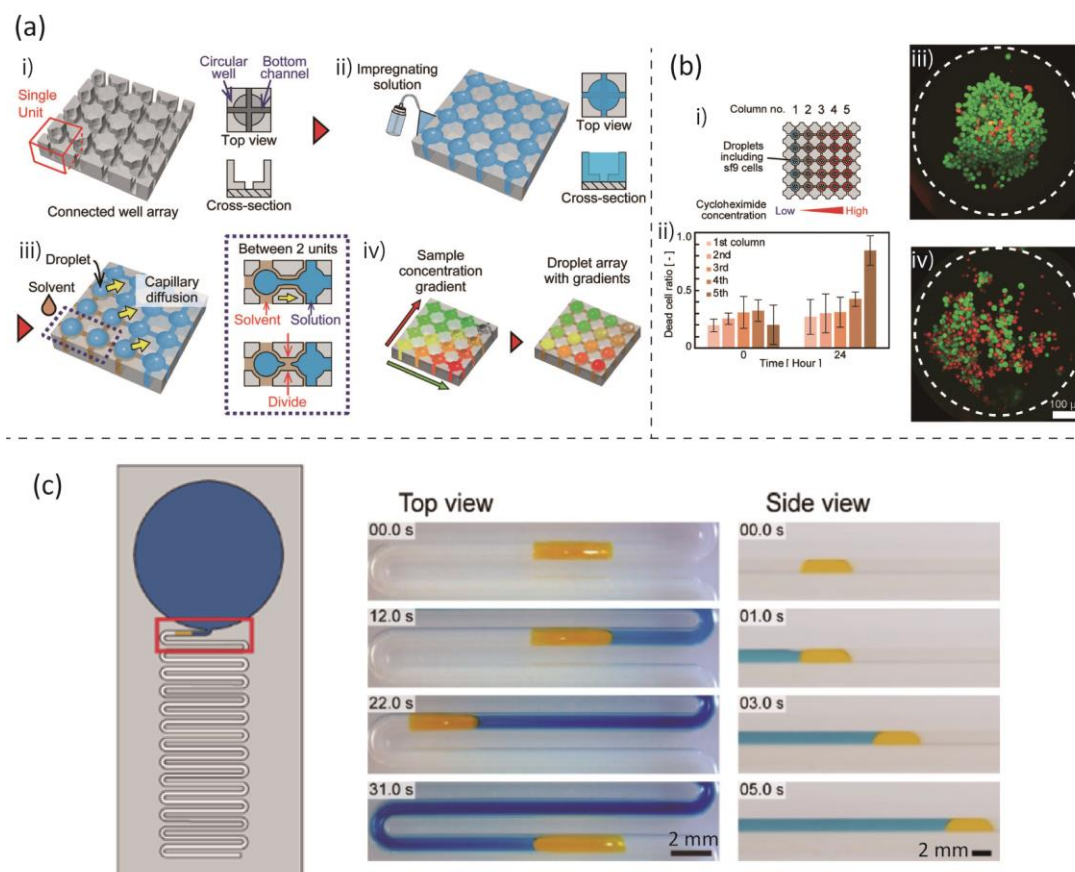
Figure 3 Systems using two-phase capillary flow in microstructure patterns. (a) Droplet-array generation in a connected well array via spontaneous replacement between oil and water: i) a connected well array, ii) impregnation of aqueous solution in the well array, iii) droplet generation by oil diffusion, and iv) formation of sample concentration gradient in a droplet array. Adapted with permission from [15]. Copyright 2018 The Royal Society of Chemistry. (b) A live–dead cell assay in a droplet array: i) concentration gradient of cycloheximide in a droplet array, ii) dead cell ratio at 0 an 24 hours after incubation, iii) cell viability in a droplet with low concentration of cycloheximide, (the droplet included red colored dead cells and green colored live cells), and iv) cell viability in a droplet with high concentration of cycloheximide. Adapted with permission from [15]. Copyright 2018 The Royal Society of Chemistry. (c) Droplet transport by capillary flow of a droplet (yellow) in a flow of another type of liquid immiscible (blue) to the droplet. Adapted with permission from [35]. Copyright 2018 American Chemical Society.
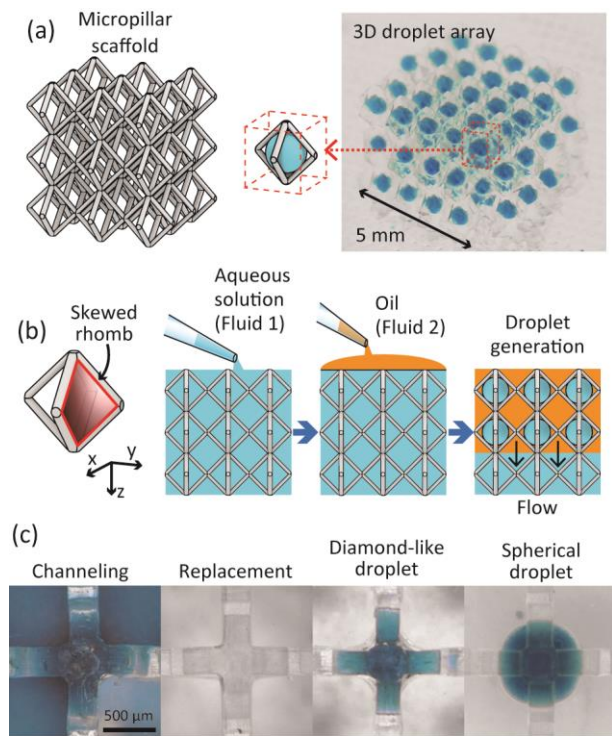
in 3D templates are also required. Our recent study founded a key approach termed as FLUID3EAMS that satisfies both requirements.

An overview of FLUID3EAMS is shown in Figs. 4(a) and (b). FLUID3EAMS refers to the phenomenon in which the interface of two immiscible fluids (defined as fluids 1 and 2, such as water and oil) passes through a 3D microscaffold structure and fluid 1, which is filled in advance, is spontaneously split and arrayed into microdroplets. FLUID3EAMS gives rise to microscale periodic structures, including three elements: a continuous microscaffold solid, a 3D array of dispersed fluid 1 particles inside fluid traps, and a continuous fluid 2 that fills the remaining void.

There exist two requirements to generate microdroplets using FLUID3EAMS. The first requirement is related to the filling condition, where the interfacial energy dominates other effects and the two fluids have the same viscosity. The second requirement is related to "fluid trap" geometries that must occur in every lattice unit cell of the scaffold structure. Here, a fluid trap is introduced with a focus on the scaffold structure consisting of octahedrally connected micropillar lattices. The general principle of the fluid trap is presented in the literature [17]. When the fluid interface passes along the axial direction of the lattice (Z direction in Fig. 4(b)), to enter the region inside the octahedron, the liquid 2 front must pass through at least one of the four skewed squares (red frame on the left side of Fig. 4(b)). In this region, a characteristic pressure barrier exists at the interface with curvature. If the pressure barrier exceeds the pressure for the liquid 2 front to continue along the lattice symmetry axis, a droplet of fluid 1 remains in the trap.

The near-ideal conditions for droplet generation by FLUID3EAMS were evaluated through experiments and fluid simulations with three dimensionless numbers: Ca (Ca = $\mu_2 u/\gamma$: capillary number), $\cos\theta$ (θ represents the static contact angle of fluid 1 and fluid 2), and μ_2/μ_1 (viscosity ratio), where μ_1 and μ_2 represent the viscosities of fluids 1 and 2, respectively; u represents the mean velocity of the interface propagation; and γ represents the interfacial tension between fluids 1 and 2. In the experiment, fluid 1 was a glycerol aqueous solution, and fluid 2 was a mineral oil-containing surfactant (Span80). From these evaluations, four characteristic modes were confirmed, including two modes with droplet generation (Fig. 4(c)). The first mode in which droplets could not be generated was channeling. The channeling was mainly observed at small Ca values and $\cos\theta > 0$. The channeling was likely to occur as follows. Because the structure surface was more wettable by fluid 1, when fluid 2 reached the structure, fluid 2 was not possible to push fluid 1 out of the structure completely. As a result, fluid 2 formed a channel only in part of fluid 1 filled in the scaffold. In the second mode, fluid 1 filled in the scaffold was completely replaced by fluid 2. The replacement mode was observed at $\cos\theta < 0$ and small Ca values, that is, when the structure was more wettable by fluid 2.

Droplets with two different shapes were observed. First, diamond-like droplets generated from fluid 1 were pinned to octahedral pillars. The diamond-like droplets were observed over a wide range of Ca values under the condition of $-0.4 < \cos\theta < 0.2$. As mentioned previously, it is likely that a pressure barrier was formed around the octahedral region, and consequently, the droplet remained in the fluid trap after the interface passed through the scaffold. The second droplet shape was

Figure 4 Generation of a 3D microdroplet array by FLUID3EAMS. (a) Schematic of a micropillar scaffold (left) and a photograph of a generated 3D droplet array (right). (b) Schematics of an octahedral region inside a microscaffold functioning as a fluid trap and the basic principle of FLUID3EAMS. (c) Four modes after the interface passing through a microscaffold under different fluid and microstructural conditions. Adapted with permission from [17]. Copyright 2021 Springer Nature.

spherical. Spherical droplets were observed under $\cos\theta < 0$ and large Ca values. In this mode, diamond-like droplets of fluid 1, which were first generated in the octahedral region, were unpinned from the micropillar because the scaffold was more wettable by fluid 2, and the droplets became spherical through the minimization of the surface energy. These droplet shapes were confirmed experimentally and through fluid simulations performed using similar parameters. Among the aforementioned cases, when $\cos\theta$ was < 0, the generation of spherical droplets was observed even after spontaneous replacement from fluid 1 to fluid 2. This indicated that the spontaneous generation of a 3D droplet array is possible based on capillarity without external fluid manipulation using a syringe pump or pressure pump (Fig. 4(a), right). Furthermore, this method allows fast droplet generation. Droplets can be generated at a flow velocity of $u \approx 10$ mm/s; thus, a large number of droplets can be generated in a short time by increasing the scale of the scaffold.

Fabrication of Microscaffold Structures and Tunability of Size of Droplets Generated by FLUID3EAMS

A 3D microscaffold structure must include a fluid trap for droplet generation by FLUID3EAMS. In our study, multidirectional photolithography and 3D printing were used for fabricating such microscaffold structures. Multidirectional photolithography is photolithography using ultraviolet (UV) light from multiple directions. As shown in Fig. 5(a), a 3D microscaffold structure was fabricated by exposing the photocurable resin to UV light from multiple directions through a photomask printed with a pattern of micropillars [40,41].

Regarding the selection of materials, a UV-curable polymer system that can modify the surface energy of scaffolds is preferable. In our previous study [17], a UV-curable polymer system called off-stoichiometry thiol-ene (OSTE) was selected as the material, which is suitable for the modification of the surface energy [42]. The major constituents of OSTE are two monomers—one containing thiol groups and the other containing ene (allyl) groups. The total amount of either the thiol or ene group was intentionally larger than that of the other, resulting in a surface containing unreacted functional

groups after polymerization. The OSTE polymer surface, including thiol groups, can be modified by rapid photografting onto hydrophilic/hydrophobic surfaces [43] or protein-immobilized surfaces [44]. Hansson et al. fabricated a micropillar scaffold based on OSTE for the first time, which was called "synthetic (microfluidic) paper" [19]. Fig. 5(b) shows the synthetic paper composed of slanted and mutually interconnected straight micropillars. Because of this structural feature, the synthetic paper is robust against mechanical collapse. Furthermore, the synthetic paper has a large specific surface area, making the synthetic paper advantageous for biosensing or bioassays. Microfluidic devices based on synthetic paper have been developed for various applications, such as immunoassays and lateral flow tests [45,46]. In addition, Kamiya et al. demonstrated that synthetic paper strips can be used as dipsticks to sample liquids [47].

FLUID3EAMS allows droplet generation on a variable scale, depending on the size of the fluid trap in the 3D scaffold structure. Droplet generation was demonstrated from 1 mm (Fig. 4(a)) to 20 μm (Fig. 5(c)) on the unit length scale of the fluid trap. In addition, it was possible to increase the number of droplets generated by changing the area and thickness of the fabricated microscaffold structure. Droplet generation on the cm^2 scale was demonstrated [17].
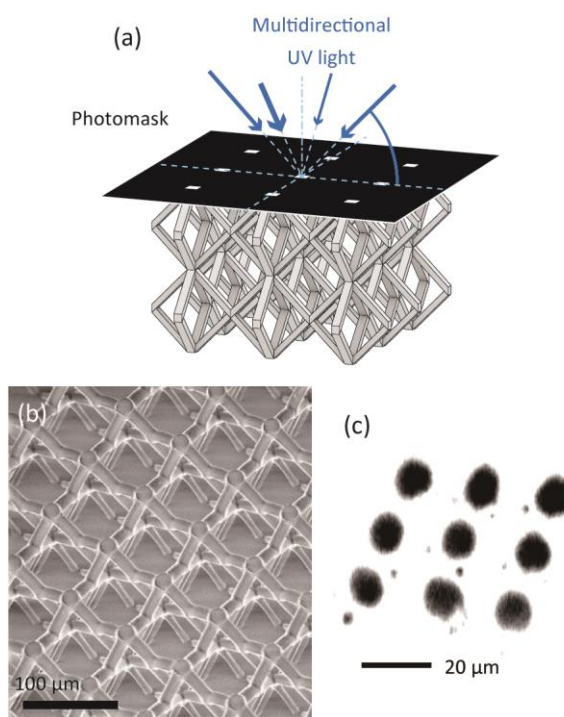
The 3D arrangement of the droplets generated by FLUID3EAMS was determined by the morphology of the microscaffold structure. Multidirectional photolithography can produce only a few types of microscaffold structures, and the 3D array pattern of microdroplets is limited to these structures [17]. In addition, as long as the fluid and the interface behave as a

Figure 5 Micropillar scaffolds for capillary-based microfluidic devices and droplet generation. (a) Schematic of multidirectional photolithography. (b) Scanning electron microscope image of fabricated synthetic paper. Adapted with permission from [19]. Copyright 2016 The Royal Society of Chemistry. (c) Confocal microscope image of generated 10-μm-scale droplets. Adapted with permission from [17]. Copyright 2021 Springer Nature.

continuum, the size of the generated droplets can be miniaturized to the nanoscale (10–10^2 nm), but this is limited to the scale at which microscaffold structures can be fabricated using the current fabrication methods. In fact, the scale of the scaffold remained at 10 μm, which is the empirical fabrication limit for multidirectional photolithography. However, droplets can be generated in a microscaffold structure manufactured using a 3D printer [17]. In the near future, 3D printers are expected to enable the generation of 3D droplet arrays with arbitrary morphologies and further miniaturization of the droplet size, for example, with the use of two-photon microstereolithography with a scale resolution of approximately 100 nm [48].

Application of FLUID3EAMS

Microdroplet arrays generated by FLUID3EAMS have various potential applications, and several applications have been demonstrated [17]. Here, the formation of composite structures, including droplet arrays with different material phases, tissue-like network formation of microdroplets via artificial cell membranes, and encapsulation of highly dense cells in droplets are introduced.

Because the droplet arrays generated by FLUID3EAMS have a state of spatial separation, the risk of coalescence of the droplets is negligible, and the droplets are kept stable without the use of surfactants. Taking advantage of this feature, as the first application, composite structures containing droplets and the surrounding solution in different phases have been fabricated by changing the phases of fluids 1 and 2 to solid (gel or polymer), liquid, and gas. Hydrogelation or polymerization of the liquid phases was employed to form composite structures, including solid phases (Fig. 6(a)).

The second application is 3D droplet interface bilayer (DIB) network formation. The DIB network is a tissue-like network composed of water-in-oil droplets whose droplets are connected by lipid bilayers. Generally, it is difficult to assemble a 3D array of droplets forming a DIB network in an arbitrary arrangement. Droplet arrays generated in a microscaffold structure by FLUID3EAMS can be applied to overcome this challenge; single-layered 2D droplet arrays

are generated by FLUID3EAMS and then stacked to form a 3D DIB network. The 3D arrangement of droplets can be defined by the mechanical immobilization of droplets in microscaffold structures. Furthermore, the advantage of this method lies in its ability to pattern the solution composition in 3D by patterning reagents to droplets in the individual 2D array before stacking (Fig. 6(b)).

Finally, the formation of hydrogel beads containing highly dense cells was demonstrated. Compared with ordinary microfluidic droplet generators, FLUID3EAMS allowed droplet generation with relatively low shear, resulting in the encapsulation of denser cells into droplets. Subsequent hydrogelation converted the droplets into hydrogel beads, immobilizing highly dense cells (Fig. 6(c)). The generated gel beads can be released from the scaffold structure by laterally flowing oil; thus, it is possible to obtain individual hydrogel beads containing highly dense cells. The hydrogel beads containing highly dense cells are expected to contribute to cell therapy. Cell-containing hydrogel beads formed via this method have sizes on the order of 100 μm. This size is suitable for transplantation in cell therapy. Furthermore, this method is useful for cell therapy, because the density of encapsulated cells is approximately one order of magnitude higher than that for conventional methods. In addition, FLUID3EAMS has been used to form core–shell particles containing cells by forming a polymer thin film on the droplet surface.

Figure 6 Application of FLUID3EAMS. (a) Generation of droplet arrays with different material phase combinations. (b) Demonstration of the ability to pattern solution contents of droplets in a DIB network. (c) Encapsulation of highly dense cells (Glioma cell line U87) in alginate hydrogel beads. Left: general view of one gel beads. Right: enlarged view. Green fluorescence indicates actin filaments stained with Alexa Fluor 488 phalloidin, and blue fluorescence indicates nuclei stained with Hoechst. Adapted with permission from [17]. Copyright 2021 Springer Nature.

Summary

The methods for the spontaneous generation of 3D droplet arrays based on capillarity have been reviewed. Starting from the general formats of capillarity-based microfluidic devices, methods to generate droplets using two-phase flows driven by capillarity, i.e., oil–water replacement, were introduced. This review focused on a novel method based on FLUID3EAMS for generating arrays of droplets and hydrogel beads that are useful in various research fields, such as the development of periodic materials containing multiple phases, the formation of tissue-like networks, and the microencapsulation of biological cells.

The microscale 3D droplet array generated by FLUID3EAMS has a large liquid–liquid specific surface area that can theoretically reach a scale of $1 \ m^2/cm^3$. By exploiting this feature, I expect the development of a droplet-based microreactor system whose droplets enclose cells, tissues, or microorganisms with perfusion functions. In addition, this feature is of potential interest for the development of gas-adsorption materials. In future research, it will be necessary to generate droplets on a further miniaturized scale via FLUID3EAMS, which is important for digital bioassays. Currently, I and collaborators are working on the generation of submicron-scale droplets using stereolithography 3D printers and two-photon microstereolithography, and future achievements will introduce further possibilities for capillarity-based droplet systems.
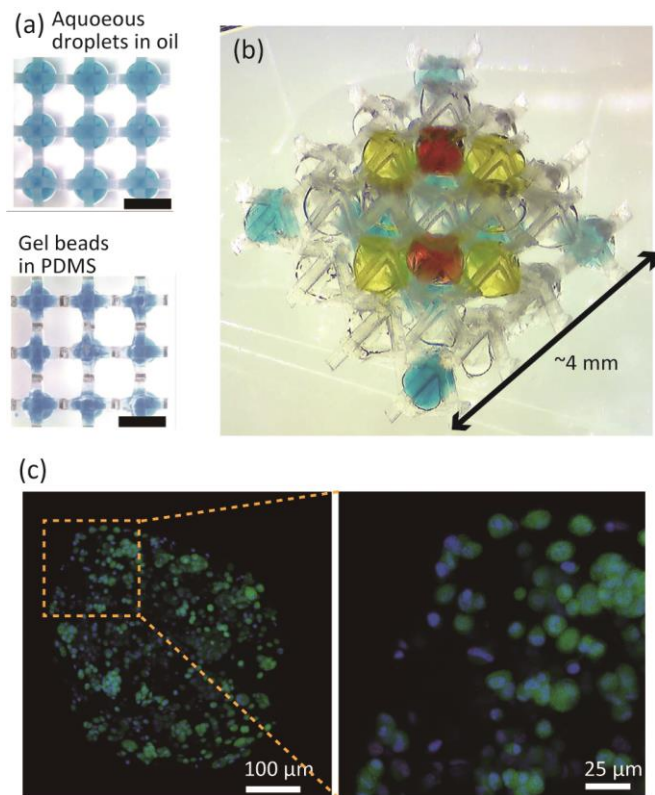
Conflict of Interest

The author declares no conflicts of interest.

Author Contributions

H.Y. wrote the manuscript.

Data Availability

The evidence data generated during the current study are available from the corresponding author on reasonable request.

References

[1] Convery, N., Gadegaard, N. 30 Years of microfluidics. Micro Nano Engineering 2, 76–91 (2019). https://doi.org/10.1016/j.mne.2019.01.003

[2] Theberge, A. B., Courtois, F., Schaerli, Y., Fischlechner, M., Abell, C., Hollfelder, F., et al. Microdroplets in microfluidics: An evolving platform for discoveries in chemistry and biology. Angew. Chem. Int. Ed. Engl. 49, 5846–5868 (2010). https://doi.org/10.1002/anie.200906653

[3] Lederberg, J. A simple method for isolating individual microbes. J. Bacteriol. 68, 258–259 (1954). https://doi.org/10.1128/jb.68.2.258-259.1954

[4] Pompano, R. R., Liu, W., Du, W., Ismagilov, R. F. Microfluidics using spatially defined arrays of droplets in one, two, and three dimensions. Annu. Rev. Anal. Chem. (Palo Alto Calif) 4, 59–81 (2011). https://doi.org/10.1146/annurev.anchem.012809.102303

[5] Courtois, F., Olguin, L. F., Whyte, G., Theberge, A. B., Huck, W. T. S., Hollfelder, F., et al. Controlling the retention of small molecules in emulsion microdroplets for use in cell-based assays. Anal. Chem. 81, 3008–3016 (2009). https://doi.org/10.1021/ac802658n

[6] Shi, W., Qin, J., Ye, N., Lin, B. Droplet-based microfluidic system for individual Caenorhabditis elegans assay. Lab Chip 8, 1432–1435 (2008). https://doi.org/10.1039/b808753a

[7] Zhu, Y., Zhang, Y. X., Cai, L. F., Fang, Q. Sequential operation droplet array: An automated microfluidic platform for picoliter-scale liquid handling, analysis, and screening. Anal. Chem. 85, 6723–6731 (2013). https://doi.org/10.1021/ac4006414

[8] Cai, L. F., Zhu, Y., Du, G. S., Fang, Q. Droplet-based microfluidic flow injection system with large-scale concentration gradient by a single nanoliter-scale injection for enzyme inhibition assay. Anal. Chem. 84, 446–452 (2012). https://doi.org/10.1021/ac2029198

[9] Cohen, D. E., Schneider, T., Wang, M., Chiu, D. T. Self-digitization of sample volumes. Anal. Chem. 82, 5707–5717 (2010). https://doi.org/10.1021/ac100713u

[10] Jackman, R. J., Duffy, D. C., Ostuni, E., Willmore, N. D., Whitesides, G. M. Fabricating large arrays of microwells with arbitrary dimensions and filling them using discontinuous dewetting. Anal. Chem. 70, 2280–2287 (1998). https://doi.org/10.1021/ac971295a

[11] Decrop, D., Pardon, G., Brancato, L., Kil, D., Zandi Shafagh, R., Kokalj, T., et al. Single-step imprinting of femtoliter microwell arrays allows digital bioassays with attomolar limit of detection. ACS Appl. Mater. Interfaces 9, 10418–10426 (2017). https://doi.org/10.1021/acsami.6b15415

[12] Pardon, G., Haraldsson, T., van der Wijngaart, W. Simultaneous replication of hydrophilic and superhydrophobic micropatterns through area-selective monomers self-assembly. Adv. Mater. Interfaces 3, 1600404 (2016). https://doi.org/10.1002/admi.201600404

[13] Ueda, E., Geyer, F. L., Nedashkivska, V., Levkin, P. A. DropletMicroarray: Facile formation of arrays of microdroplets and hydrogel micropads for cell screening applications. Lab Chip 12, 5218–5224 (2012). https://doi.org/10.1039/c2lc40921f

[14] Tonooka, T., Sato, K., Osaki, T., Kawano, R., Takeuchi, S. Lipid bilayers on a picoliter microdroplet array for rapid fluorescence detection of membrane transport. Small 10, 3275–3282 (2014). https://doi.org/10.1002/smll.201303332

[15] Yasuga, H., Kamiya, K., Takeuchi, S., Miki, N. Self-generation of two-dimensional droplet array using oil-water immiscibility and replacement. Lab Chip 18, 1130–1137 (2018). https://doi.org/10.1039/c7lc01360d

[16] Hatch, A. C., Fisher, J. S., Pentoney, S. L., Yang, D. L., Lee, A. P. Tunable 3D droplet self-assembly for ultra-high-density digital micro-reactor arrays. Lab Chip 11, 2509–2517 (2011). https://doi.org/10.1039/c0lc00553c

[17] Yasuga, H., Iseri, E., Wei, X., Kaya, K., di Dio, G., Osaki, T., et al. Fluid interfacial energy drives the emergence of three-dimensional periodic structures in micropillar scaffolds. Nat. Phys. 17, 794–800 (2021). https://doi.org/10.1038/s41567-021-01204-4

[18] Yasuga, H. FLUID3EAMS: Fluid–fluid interfacial energy driven 3D structure emergence in a micropillar scaffold and development in bioengineering. SEIBUTSU BUTSURI 62, 110–113 (2022). https://doi.org/10.2142/biophys.62.110

[19] Hansson, J., Yasuga, H., Haraldsson, T., van der Wijngaart, W. Synthetic microfluidic paper: high surface area and high porosity polymer micropillar arrays. Lab Chip 16, 298–304 (2016). https://doi.org/10.1039/C5LC01318F

[20] Berthier, J., Brakke, K. A., Berthier, E. Open Microfluidics. (John Wiley & Sons, New Jersey, 2016). https://doi.org/10.1002/9781118720936

[21] Berry, S. B., Lee, J. J., Berthier, J., Berthier, E., Theberge, A. B. Droplet incubation and splitting in open microfluidic channels. Anal. Methods 11, 4528–4536 (2019). https://doi.org/10.1039/c9ay00758j

[22] Yetisen, A. K., Akram, M. S., Lowe, C. R. Paper-based microfluidic point-of-care diagnostic devices. Lab Chip 13, 2210–2251 (2013). https://doi.org/10.1039/c3lc50169h

[23] Olanrewaju, A., Beaugrand, M., Yafia, M., Juncker, D. Capillary microfluidics in microchannels: From microfluidic networks to capillaric circuits. Lab Chip 18, 2323–2347 (2018). https://doi.org/10.1039/C8LC00458G

[24] Juncker, D., Schmid, H., Drechsler, U., Wolf, H., Wolf, M., Michel, B., et al. Autonomous microfluidic capillary system. Anal. Chem. 74, 6139–6144 (2002). https://doi.org/10.1021/ac0261449

[25] Dudek, M. M., Gandhiraman, R. P., Volcke, C., Daniels, S., Killard, A. J. Evaluation of a range of surface modifications for the enhancement of lateral flow assays on cyclic polyolefin micropillar devices. Plasma Process. Polym. 6, 620–630 (2009). https://doi.org/10.1002/ppap.200900053

[26] Zimmermann, M., Schmid, H., Hunziker, P., Delamarche, E. Capillary pumps for autonomous capillary systems. Lab Chip 7, 119–125 (2007). https://doi.org/10.1039/b609813d

[27] Mohammed, M. I., Desmulliez, M. P. Y. Autonomous capillary microfluidic system with embedded optics for improved troponin I cardiac biomarker detection. Biosens. Bioelectron. 61, 478–484 (2014). https://doi.org/10.1016/j.bios.2014.05.042

[28] Gervais, L., Delamarche, E. Toward one-step point-of-care immunodiagnostics using capillary-driven microfluidics and PDMS substrates. Lab Chip 9, 3330–3337 (2009). https://doi.org/10.1039/b906523g

[29] André, J., Okumura, K. Capillary replacement in a tube prefilled with a viscous fluid. Langmuir 36, 10952–10959 (2020). https://doi.org/10.1021/acs.langmuir.0c01612

[30] Anna, S. L., Bontoux, N., Stone, H. A. Formation of dispersions using 'flow focusing' in microchannels. Appl. Phys. Lett. 82, 364–366 (2003). https://doi.org/10.1063/1.1537519

[31] Thorsen, T., Roberts, R. W., Arnold, F. H., Quake, S. R. Dynamic pattern formation in a vesicle-generating microfluidic device. Phys. Rev. Lett. 86, 4163–4166 (2001). https://doi.org/10.1103/PhysRevLett.86.4163

[32] Washburn, E. W. The dynamics of capillary flow. Phys. Rev. 17, 273–283 (1921). https://doi.org/10.1103/PhysRev.17.273

[33] Yasuga, H., Miki, N. Adjustment of Surface Condition for Self-Generation of Droplet Array Using Oil-Water Replacement. in TRANSDUCERS 2017 - 19th International Conference on Solid-State Sensors, Actuators and Microsystems 2175–2178 (2017). https://doi.org/10.1109/TRANSDUCERS.2017.7994507

[34] Teh, S.-Y., Lin, R., Hung, L.-H., Lee, A. P. Droplet microfluidics. Lab Chip 8, 198–220 (2008). https://doi.org/10.1039/b715524g

[35] Lee, J. J., Berthier, J., Brakke, K. A., Dostie, A. M., Theberge, A. B., Berthier, E. Droplet behavior in open biphasic microfluidics. Langmuir 34, 5358–5366 (2018). https://doi.org/10.1021/acs.langmuir.8b00380

[36] Berthier, E., Dostie, A. M., Lee, U. N., Berthier, J., Theberge, A. B. Open microfluidic capillary systems. Anal. Chem. 91, 8739–8750 (2019). https://doi.org/10.1021/acs.analchem.9b01429

[37] Guo, W., Hansson, J., van der Wijngaart, W. Capillary pumping independent of the liquid surface energy and viscosity. Microsyst. Nanoeng. 4, 2 (2018). https://doi.org/10.1038/s41378-018-0002-9

[38] Guo, W., Hansson, J., van der Wijngaart, W. Capillary pumping independent of liquid sample viscosity. Langmuir 32, 12650–12655 (2016). https://doi.org/10.1021/acs.langmuir.6b03488

[39] Booth, M. J., Schild, V. R., Graham, A. D., Olof, S. N., Bayley, H. Light-activated communication in synthetic tissues. Sci. Adv. 2, e1600056 (2016). https://doi.org/10.1126/sciadv.1600056

[40] Sato, H., Houshi, Y., Otsuka, T., Shoji, S. Fabrication of polymer and metal three-dimensional micromesh structures. Jpn. J. Appl. Phys. 43, 8341–8344 (2004). https://doi.org/10.1143/JJAP.43.8341

[41] Schaedler, T. A., Jacobsen, A. J., Torrents, A., Sorensen, A. E., Lian, J., Greer, J. R., et al. Ultralight metallic microlattices. Science 334, 962–965 (2011). https://doi.org/10.1126/science.1211649

[42] Carlborg, C. F., Haraldsson, T., Öberg, K., Malkoch, M., van der Wijngaart, W. Beyond PDMS: Off-stoichiometry thiol-ene (OSTE) based soft lithography for rapid prototyping of microfluidic devices. Lab Chip 11, 3136–3147

(2011). https://doi.org/10.1039/c1lc20388f

[43] Pardon, G., Saharil, F., Karlsson, J. M., Supekar, O., Carlborg, C. F., van der Wijngaart, W., et al. Rapid mold-free manufacturing of microfluidic devices with robust and spatially directed surface modifications. Microfluid. Nanofluidics 17, 773–779 (2014). https://doi.org/10.1007/s10404-014-1351-9

[44] Sticker, D., Geczy, R., Häfeli, U. O., Kutter, J. P. Thiol-ene based polymers as versatile materials for microfluidic devices for life sciences applications. ACS Appl. Mater. Interfaces 12, 10080–10095 (2020). https://doi.org/10.1021/acsami.9b22050

[45] Guo, W., Vilaplana, L., Hansson, J., Marco, M. P., van der Wijngaart, W. Immunoassays on thiol-ene synthetic paper generate a superior fluorescence signal. Biosens. Bioelectron. 163, 112279 (2020). https://doi.org/10.1016/j.bios.2020.112279

[46] Guo, W., Hansson, J., van der Wijngaart, W. Synthetic paper separates plasma from whole blood with low protein loss. Anal. Chem. 92, 6194–6199 (2020). https://doi.org/10.1021/acs.analchem.0c01474

[47] Kamiya, H., Yasuga, H., Miki, N. Ion concentration measurement using synthetic microfluidic papers. PLoS One 15, e0242188 (2020). https://doi.org/10.1371/journal.pone.0242188

[48] Kawata, S., Sun, H. B., Tanaka, T., Takada, K. Finer features for functional microdevices. Nature 412, 697–698 (2001). https://doi.org/10.1038/35089130